Design and Fabrication of Rocketlike Tetrapodal CdS Nanorods by Seed-Epitaxial Metal–Organic Chemical Vapor Deposition

ARTICLE *in* CRYSTAL GROWTH & DESIGN · FEBRUARY 2007

Impact Factor: 4.89 · DOI: 10.1021/cg0608514

8 AUTHORS, INCLUDING:

Zhanjun Gu
Chinese Academy of Sciences
82 PUBLICATIONS **2,006** CITATIONS
SEE PROFILE

Haizheng Zhong
Beijing Institute of Technology
67 PUBLICATIONS **1,826** CITATIONS
SEE PROFILE

Ying Ma
Shandong University
427 PUBLICATIONS **8,692** CITATIONS
SEE PROFILE

Hongbing Fu
Chinese Academy of Sciences
139 PUBLICATIONS **3,205** CITATIONS
SEE PROFILE

CRYSTAL GROWTH & DESIGN
2007
VOL. 7, NO. 3
488−491

Design and Fabrication of Rocketlike Tetrapodal CdS Nanorods by Seed-Epitaxial Metal−Organic Chemical Vapor Deposition

Tianyou Zhai,[†,‡] Zhanjun Gu,[†,‡] Haizheng Zhong,[†,‡] Yang Dong,[†,‡] Ying Ma,*[,†] Hongbing Fu,[†] Yongfang Li,[†] and Jiannian Yao*[,†]

Beijing National Laboratory for Molecular Sciences (BNLMS), Institute of Chemistry, Chinese Academy of Sciences, Beijing 100080, P.R. China, and Graduate School, Chinese Academy of Sciences, Beijing 100039, P.R. China

Received November 28, 2006; Revised Manuscript Received January 15, 2007

ABSTRACT: Single-crystalline rocketlike tetrapodal CdS nanorods were synthesized via a one-step seed-epitaxial MOCVD approach by thermal decomposition of $Cd(S_2CNEt_2)_2$ powders. This bottom-up method uses silver particles to initiate and guide the preferential orientation of the axial nanorods, whereas the epitaxial growth of wurtzite-structured branches occurs on the cubic CdSe seeds. This controlled seed-epitaxial method has potential as a general means of forming complex branching structures and may also offer opportunities for applications as building blocks for optoelectronic devices.

Significant efforts have been made to control the size and shape of inorganic nanocrystals, because these parameters primarily determine their electronic and optical properties.[1−5] One way to achieve shape control is to enhance anisotropic nanocrystals growth using a liquid medium such as the vapor−liquid−solid (VLS) method.[6] Another common approach is to use surfactants or micelles (regular or inverse) as regulating agents or templates to facilitate anisotropic crystal growth.[7−9] More recently, complicated nanostructures, such as tetrapodlike, hierarchical, dendritic, etc., are highly desired considering their applications as interconnections in the "bottom-up" self-assembly approach toward future nanocircuits and nanodevices. Among them, tetrapodal branched nanostructures are typical because they present promising properties in field emission, mechanical reinforcement of polymer, infrared adsorption, photovoltaic devices, and so on.[10−15] Until now, tetrapodal crystals have frequently occured in several materials such as ZnO,[6] ZnS,[16] ZnSe,[2] CdS,[17] CdSe,[18] and CdTe,[10,19] which are generated through epitaxial growth of wurtzite-structured arms out of the zinc-blende-phased core.[20] In all above cases, however, harsh conditions such as reactions in organic solvents or chemical vapor deposition at high temperatures are normally required. Obviously, seeking new and versatile synthetic routes may be very important.

In forming the tetrapodal structure, phase control and switching (nucleation in the zinc blende phase while growing in the wurtzite phase) are key steps. To control these steps, it is necessary to change the nucleation and growth environments and separate the nucleation and growth processes,[21] and the epitaxial growth has long been regarded as the best strategy. Epitaxial growth, however, usually takes place two-dimensionally on a planar substrate; recently, it has been built three-dimensionally on the nanowire surfaces between two materials with the same crystal structure.[22] In addition, the epitaxial growth of wurtzite layers out of a tetrahedral zinc core has been observed before.[23] The growth of these self-assembled nanoarchitectures is based on the crystallographic characteristics. This motivated us to design and fabricate 3D CdS nanoarchitectures. It is well-known that zinc blende CdSe and wurtzite CdS have similar crystal structures and close lattice constants. In accordance with the lattice-matching theory, effective epitaxial growth of CdS on CdSe substrates should be possible, because the CdSe−CdS core−shell nanostructures have already been demonstrated.[24,25] Borrowing the idea of epitaxial growth, we fabricate here the rocketlike tetrapodal CdS nanorods (RTPs) via a one-step seed-epitaxial metal−organic chemical vapor deposition (MOCVD) approach by thermal decomposition of $Cd(S_2CNEt_2)_2$ powders. This bottom-up method uses silver particles to initiate and guide the preferential orientation of the axial nanorods, whereas the epitaxial growth of wurtzite-structured branches occurs on the cubic CdSe seeds. We show, by high-resolution transmission electron microscopy, that the branching mechanism gives continuous crystalline structure throughout the complex rocketlike structures. In addition, because of the lower temperature and versatility, this new controlled seed-epitaxial method has potential as a general means of forming complex branching structures and may also offer opportunities for applications as building blocks for optoelectronic devices.

The CdS RTPs were synthesized through a low-pressure thermal decomposition process described previously.[26−28] Homemade $Cd(S_2CNEt_2)_2$ powders were placed at the upstream end of the tube furnace and evacuated for several hours to purge oxygen in the chamber. After the elevation process was complete, the system was heated to 420 °C in 30 min and kept at this temperature for 60 min in a flowing atmosphere of N_2, which serves as both protecting medium and a carrying gas. During the heating process, the N_2 flow rate and pressure were kept at 20 sccm and 65 Pa, respectively. Single-crystal silicon substrates covered first with silver particles and then dispersed with cubic CdSe nanocrystals with typical sizes of 4−5 nm, prepared according to literature methods[29,30] (see the Supporting Information for details), were used for growing the nanostructures. The substrates were placed at the central high-temperature zone to collect the deposited CdS nanostructures. After the furnace was cooled to room temperature, the products were characterized by powder X-ray diffraction (XRD, Rigaku D/max-2400PC), scanning electron microscopy (SEM, Hitachi F-4300) equipped with energy-dispersive X-ray spectrometry (EDS), and transmission electron microscope (TEM, JEOL JEM-2010 and HRTEM, Philips Tecnai F-30).

The as-synthesized product was first analyzed by scanning electron microscopy (SEM). Optically, it appears gray and covers the silicon deposition substrate. The synthesized material has a relatively high yield on the substrate and shows a high degree of reproducibility. The deposited material has a dominant morphology, i.e., rocketlike tetrapodal CdS nanorods. Each nanorod consists of three branches of 500 nm in length, and the axis nanorod of diameter 200 nm. The nanorods remain their threefold array of parallel branches around the central nanorods. The magnified image (Figure 1b) shows some rougher stepped surfaces of the axis rod than the flat smooth surfaces of the branches. Unlike the traditional tetrapodal structure, the central rod was longer than the branches and passed through the center of the tetrapod. These structural characters were easily noticed by the TEM image (Figure 3a). We also observed that the morphology of the CdS RTPs were sensitive to several experimental conditions, such as reaction temperature, deposition time, and carries gas rate, similar to the typical chemical

* To whom correspondence should be addressed. Phone/Fax: 86-10-82616517. E-mail: yingma@iccas.ac.cn (Y.M.); jnyao@iccas.ac.cn (J.Y.).
[†] Institute of Chemistry, Chinese Academy of Sciences.
[‡] Graduate School, Chinese Academy of Sciences.

10.1021/cg0608514 CCC: $37.00
Published on Web 02/14/2007

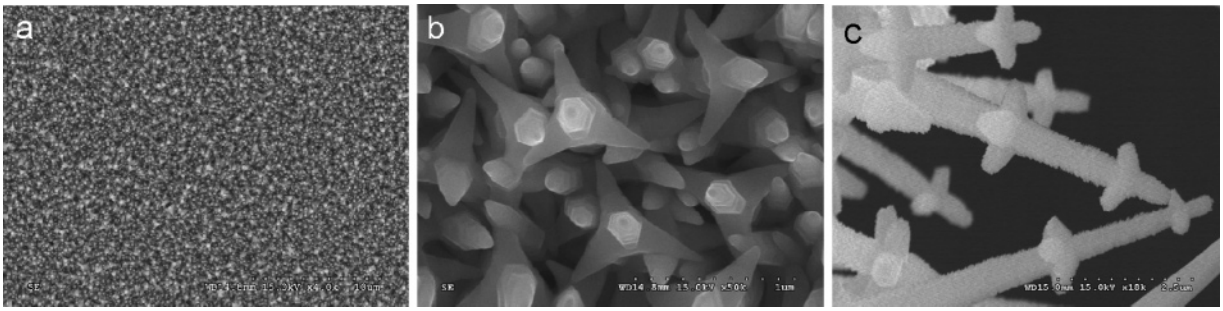

Figure 1. (a) Low-magnification SEM image of the as-deposited CdS products; (b) high-magnification SEM image clearly revealing the rocketlike tetrapodal nanorods architectures; (c) SEM image of two-level RTPs.

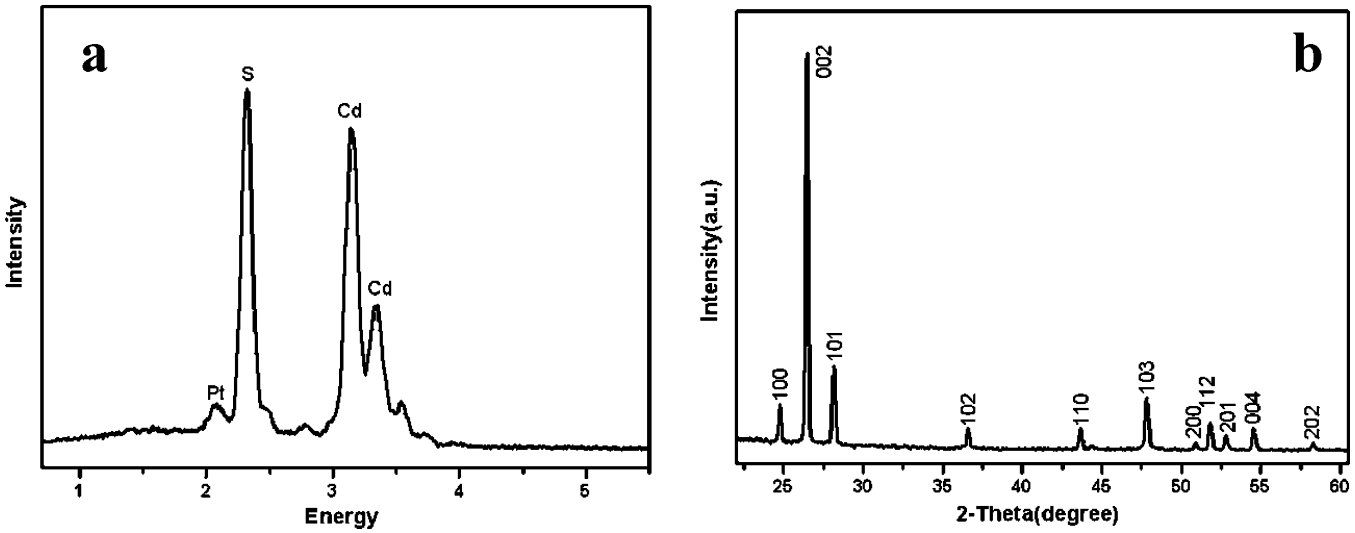

Figure 2. (a) EDS spectrum and (b) XRD pattern of the deposited CdS RTPs, showing the formation of the CdS product.

vapor deposition technique (see the Supporting Information), possibly because of their preferential growth, as explained later. Furthermore, we found other interesting structure morphologies of CdS crystallites at the side of the substrates as shown in Figure 1c, which can be called two-level RTPs. The in situ EDS analysis confirms that the composition of CdS RTPs is stoichiometric with negligible signals from CdSe (Figure 2a). An X-ray powder diffraction pattern (Figure 2b) indicates that these nanostructures possess a hexagonal (wurtzite) CdS with the lattice parameters of $a = 4.140$ Å and $c = 6.719$ Å (JCPDS: 41-1049).

Transmission electron microscopy (TEM) provides further information on the nanostructure growth. Images a and b of Figure 3 display two low-magnification TEM images of the same CdS RTPs, which were taken when the sample plane was horizontal and tilted to another angle, in which one branch is nearly overlapped, so that the structure appears as if it has only two branches. Detailed structure analysis of the as-synthesized CdS nanorod was performed with high-resolution TEM (HRTEM) and electron diffraction (ED). Figure 3c is an HRTEM image of the central axial nanorod within the architecture. The lattice fringes of the {010} and {001} planes are clearly seen with d spacings of ~0.36 and ~0.67 nm, respectively, which are characteristics of the wurtzite CdS crystal structure. Notably, the elongated spots of the ED pattern (inset of Figure 3c) originate from the axial nanorod, which intersects the Eward's sphere of reflection for the ED spots. As can be derived from the ED pattern and HRTEM image, the nanorod has a single-crystalline structure and grows along the [001] direction. Figure 3d is a HRTEM image of the interface between the branch and the central nanorod of the CdS RTPs. They all grow along the [001] crystallographic axis. The two parts display the same characteristic lattice images, indicating that they are assembled through the micro-twin relationship; the angle between the corresponding (001) planes that meet at the boundary is around 60°. All attempts to obtain suitable lattices of cubic CdSe core have proven unsuccessful because the CdSe core was buried too deep in the complex structure to obtain HRTEM images.

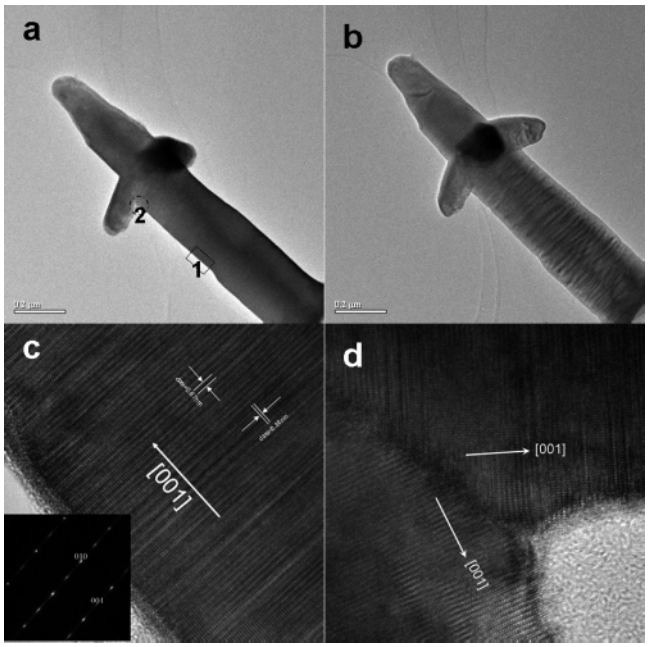

Figure 3. (a, b) TEM images of the same CdS nanorod architecture, which were taken when the sample plane was horizontal and tilted at another angle; (c, d) HRTEM images and ED pattern recorded in different regions in (a).

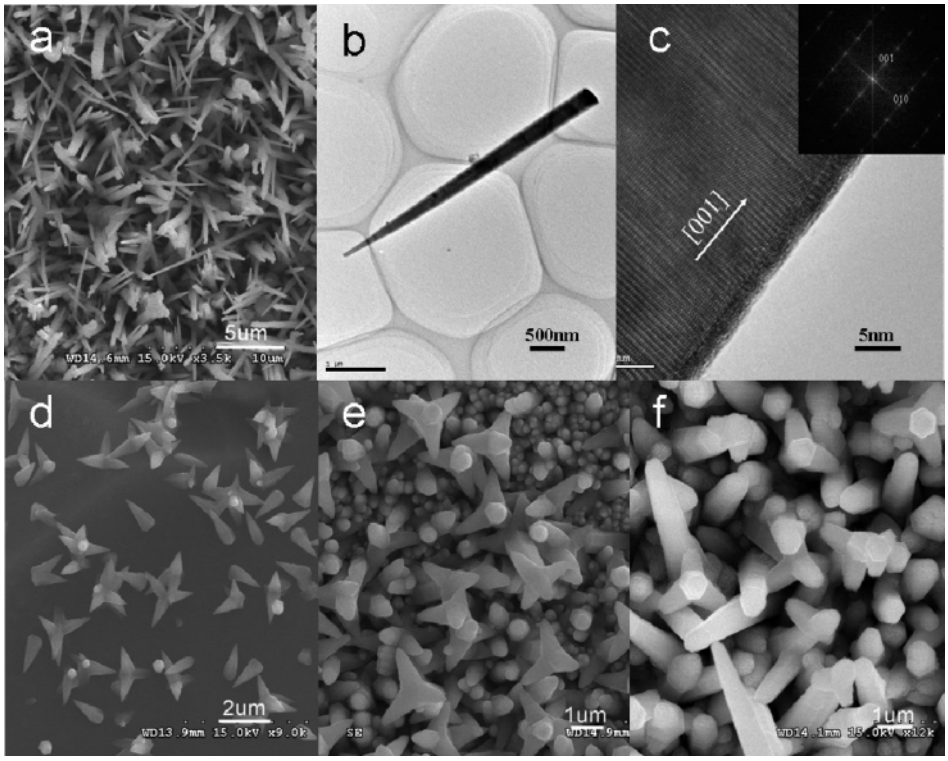

Figure 4. (a) SEM image, (b) TEM image, (c) HRTEM image and corresponding FFT pattern of CdS nanoneedles synthesized using only silver particles; SEM images of CdS nanostructures synthesized (d) using only cubic CdSe NCs, (e) using half of the silver particles used in (a) and cubic CdSe NCs, (f) using as many silver particles as used in (a) and mixed structures of CdSe NCs (wurtzite/zinc blende ≈ 2).

To understand the formation mechanism of the CdS RTPs, we have conducted additional experiments that indicate that the silver particles and cubic CdSe NCs play important roles in the formation of the CdS RTPs. Images a and d of Figure 4 show the SEM images using only silver particles and cubic CdSe NCs, respectively. When only silver particles are used, as shown in Figure 4a, high-density CdS nanoneedles cover the entire substrate. Low-magnification TEM image shows the general morphology of the individual nanoneedle. Although the lower part of the CdS nanoneedle shows uniform diameters along the nanoneedle stem, its tip exhibits the sharp morphology. No metal clusters are observed on the needle tips and no branches on the nanoneedles. HRTEM and its corresponding FFT pattern indicate that the needle is single-crystalline and grows in the [001] direction. The morphology and intrinsic structure are similar to the axis rod of the CdS RTPs. When only cubic CdSe NCs are used, some branched CdS nanostructures are obtained, similar to the branches of the RTPs. In our experiments, when the amounts of silver particles were decreased, the quantity of the CdS RTPs was reduced accordingly (Figure 4e). To confirm the importance of the zinc blende CdSe seeds in the preparation of the RTPs, we also performed controllable experiments starting from wurtzite or mixed structures of CdSe NCs. Using wurtzite NCs, we obtained CdS nanoneedles that showed a morphology similar to that formed in the absence of the seeds. Using mixed NCs, we obtained CdS nanoneedles and RTPs (Figure 4f), simultaneously, that is, no arms were observed on some CdS nanorods. These results indicate that silver particles and the zinc blende CdSe seeds are crucial to the preparation of CdS RTPs using the seed-epitaxial method.

On the basis of the above analysis, the formation process of the CdS RTPs can be proposed, a schematic description of which is given in Figure 5. At the beginning, the $Cd(S_2CNEt_2)_2$ vapor generated by thermal evaporation is transported by the carrier gas to the substrates located in a high-temperature zone and then decomposed to form CdS vapor. Meanwhile, the rough silver islands on the substrates serve as energetically preferred adsorption sites for the incoming vapor CdS, for condensation and nucleation. When

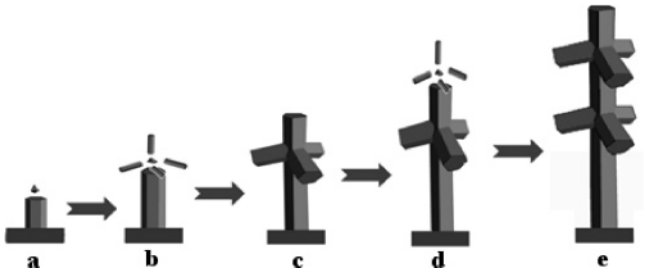

Figure 5. Schematic diagram of the growth process mechanism of the rocketlike tetrapodal CdS nanocrystals: (a) CdS nanorod formed by the silver catalysis; (b) epitaxial growth of wurtzite-structured arms on the CdSe seeds; (c) perfect CdS RTPs formed; (d) some CdSe NCs blown on the tip of RTPs, and then epitaxial growth of arms similar to (b); (e) CdS two-level RTPs formed.

the concentration of CdS reaches supersaturation, CdS precipitates and crystallizes along a certain lattice direction of low Miller index. For wurtzite CdS, it is intrinsically an anisotropic material with a unique *c*-axis. The hexagonal CdS crystal can be described as a stacking of $\{CdS_4\}$ tetrahedrally by sharing the common corners and each tetrahedron having a corner in the [001] direction.[31] The atom at the corner of a tetrahedron has the strong bonding force ($s = 2$ v.u.), compared with the atoms at other positions,[32,33] which favors the growth of CdS nanorods along the [001] axis. So the CdS will grow into rod-shaped structures along the *c*-axis. Because no metal catalysts are found, the growth is different from the traditional vapor−liquid−solid mechanism.[34] The nanorods were suggested to nucleate via a self-catalyzed mechanism. Meanwhile, with further progression in the growth due to the need for excess energy for nucleation, the newly arrived CdS vapor prefers to adsorb on seeds that exist on the CdS nanorod. The formed CdS nanocrystals should be wurtzite phase, and epitaxial growth of wurtzite-structured arms occurs on the seeds. This behavior is well-known and due to the small energy difference between stacking sequences in the growth direction. As the growth time increases,

the CdS RTPs are finally formed. When other CdSe NCs are transported and adsorb on the tips of CdS RTPs from other places, the branches grow again and finally form the two-level RTP structures.

In summary, the rocketlike tetrapodal CdS nanorods have been synthesized for the first time via a one-step seed-epitaxial MOCVD approach using Ag particles as catalysts and cubic CdSe NCs as seeds. In the growth processes, the Ag catalyst particles initiate and guide the preferential orientation of the axis nanorods, whereas epitaxial growth of wurtzite-structured arms occurs on the CdSe seeds. The specific structure may have extended the 3D architectures family and would have potential applications in nanoelectronics and photonics in the future. Although the detailed growth mechanism requires more systematic investigations, the present results suggest that this simple method might be useful for the synthesis of many other complex semiconductor nanostructures to meet the growing demands of nanoscale science and technology.

Acknowledgment. This work was supported by National Natural Science Foundation of China (50221201, 90301010, 50502033), the Chinese Academy of Sciences, and the National Research Fund for Fundamental Key Projects No. 973 (2006CB806200).

Supporting Information Available: Full experimental details; other SEM images of the RTPs, and characterization of the cubic CdSe nanocrystals. This material is available free of charge via the Internet at http://pubs.acs.org.

References

(1) Peng, X. G.; Manna, L.; Yang, W. D.; Wickham, J.; Scher, E.; Kadavanich, A.; Alivisatos, A. P. *Nature* **2000**, *404*, 59.
(2) Hu, J. Q.; Bando, Y.; Gelberg, D. *Small* **2005**, *1*, 95.
(3) Zhu, Y. C.; Bando, Y.; Yin, L. W. *Adv. Mater.* **2004**, *16*, 331.
(4) Ahmadi, T. S.; Wang, Z. L.; Green, T. C.; Henglein, A.; EI-sayed, M. A. *Science* **1996**, *272*, 1924.
(5) Shen, G. Z.; Chen, D. *J. Am. Chem. Soc.* **2006**, *128*, 11762.
(6) Yan, H. Q.; He, R. R.; Pham, J.; Yang, P. D. *Adv. Mater.* **2003**, *15*, 402.
(7) Li, M.; Schnablegger, H.; Mann, S. *Nature* **1999**, *402*, 393.
(8) Puntes, V. F.; Krishnan, K. M.; Alivisatos, A. P. *Science* **2001**, *291*, 2115.
(9) Milliron, D. J.; Hughes, S. M.; Cui, Y.; Manna, L.; Li, J. B.; Wang, L. W.; Alivisatos, A. P. *Nature* **2004**, *430*, 190.
(10) Carbone, L.; Kudera, S.; Carlino, E.; Parak, W. J.; Giannini, C.; Cingolani, R.; Manna, L. *J. Am. Chem. Soc.* **2006**, *128*, 748.
(11) Peng, Q.; Zhao, L. J.; Cai, Y.; Nguyen, D. P.; Regnault, N.; Wang, N.; Yang, S. H.; Ge, W. K.; Ferreira, R.; Bastard, G.; Wang, J. N. *Chem. Mater.* **2005**, *17*, 5263.
(12) Manna, L. D.; Milliron, J.; Meisel, A.; Scher, E. C.; Alivisatos, A. P. *Nat. Mater.* **2003**, *2*, 382.
(13) Liu, H. T.; Alivisatos, A. P. *Nano Lett.* **2004**, *4*, 2397.
(14) Gong, J. F.; Yang, S. G.; Huang, H. B.; Duan, J. H.; Liu, H. W.; Zhao, X. N.; Zhang, R.; Du, Y. W. *Small* **2006**, *2*, 732.
(15) Zhang, D. S.; Yin, Z. L.; Zhang, W. M.; Tan, X. J.; Sun, S. X. *Cryst. Growth Des.* **2006**, *6*, 1733.
(16) Zhu, Y. C.; Bando, Y.; Xue, D. F.; Golberg, D. *J. Am. Chem. Soc.* **2003**, *125*, 16196.
(17) Chen, M.; Xie, Y.; Lu, J.; Xiong, Y. J.; Zhang, S. Y.; Qian, Y. T.; Liu, X. M. *J. Mater. Chem.* **2002**, *12*, 748.
(18) Manna, L.; Scher, E. C.; Alivisatos, A. P. *J. Am. Chem. Soc.* **2000**, *122*, 12700.
(19) Yu, W. W.; Wang, Y. A.; Peng, X. G. *Chem. Mater.* **2003**, *15*, 4300.
(20) Chen, S.; Wang, Z. L.; Ballato, J.; Foulger, S. H.; Carrol, D. L. *J. Am. Chem. Soc.* **2003**, *125*, 16186.
(21) Li, Y. C.; Zhong, H. Z.; Li, R.; Zhou, Y.; Yang, C. H.; Li, Y. F. *Adv. Funct. Mater.* **2006**, *16*, 1705.
(22) Kaung, Q.; Jiang, Z. Y.; Xie, Z. Y.; Lin, S. C.; Lin, Z. W.; Xie, S. Y.; Huang, R. B.; Zheng, L. S. *J. Am. Chem. Soc.* **2005**, *127*, 11777.
(23) News, A.; Kadavanich, A. V.; Banin, U.; Alivisatos, A. P. *Phys. Rev. B: Condens. Matter* **1996**, *53*, 13242.
(24) Li, J. J.; Wang, Y. A.; Guo, W.; Keay, J. C.; Mishima, T. D.; Johnson, M. B.; Peng, X. *J. Am. Chem. Soc.* **2003**, *125*, 12567.
(25) Talapin, D. V.; Koeppe, R.; Götzinger, S.; Kornowski, A.; Lupton, J. M.; Rogach, A. L.; Benson, O.; Feldmann, J.; Weller, H. *Nano Lett.* **2003**, *3*, 1677.
(26) Barrelet, C. J.; Wu, Y.; Bell, D. C.; Lieber, C. M. *J. Am. Chem. Soc.* **2003**, *125*, 11498.
(27) Zhai, T. Y.; Gu, Z. J.; Yang, W. S.; Zhang, X. Z.; Huang, J.; Zhao, Y. S.; Yu, D. P.; Fu, H. B.; Yao, J. N. *Nanotechnology* **2006**, *17*, 4644.
(28) Zhai, T. Y.; Zhang, X. Z.; Yang, W. S.; Ma, Y.; Wang, J. F.; Gu, Z. J.; Yu, D. P.; Yang, H.; Yao, J. N. *Chem. Phys. Lett.* **2006**, *427*, 371.
(29) Peng, Z. A.; Peng, X. G. *J. Am. Chem. Soc.* **2002**, *124*, 3343.
(30) Peng, Z. A.; Peng, X. G. *J. Am. Chem. Soc.* **2001**, *123*, 183.
(31) Zhu, Y. C.; Bando, Y.; Xue, D. F.; Golberg, D. *Adv. Mater.* **2004**, *16*, 831.
(32) Xue, D.; Zhang, S. *Chem. Phys. Lett.* **1998**, *287*, 503.
(33) Brown, I. D.; Altermatt, D. *Acta Crystallogr., Sect. B* **1985**, *41*, 244.
(34) Fan, H. J.; Fuhrmann, B.; Scholz, R.; Himcinschi, C.; Serger, A.; Leipner, H.; Dadger, A.; Krost, A.; Christiansen, S.; Gösele, U.; Zacharias, M. *Nanotechnology* **2006**, *17*, S231.

CG0608514